XI. PHYSICAL ACOUSTICS*

Academic and Research Staff

Prof. K. U. Ingard
Dr. C. Krischer

Graduate Students

A. G. Galaitsis
G. F. Mazenko
P. A. Montgomery
R. M. Spitzberg

RESEARCH OBJECTIVES

Our general objective involves the study of the emission, propagation, and adsorption of acoustic waves in matter. Specific areas of present research include (i) the interaction of waves with coherent light beams in fluids and solids, (ii) dispersion of sound in semiconductors in the presence of an electric field, (iii) nonlinear acoustics in fluids, and (iv) the generation and propagation of sound waves in flowing plasmas. The last field of research includes a study of the density fluctuations in supersonic jets.

K. U. Ingard

A. THE POSSIBILITY OF RESONANCE DISPERSION OF HYPERSONIC WAVES IN LIQUIDS

Measurement of the dynamic compressibility of liquids and acoustic dispersion in the kilomegacycle frequency regime, using the technique of Brillouin scattering of laser light, is a very active area of research at present, and numerous liquids have been studied. In this report we wish to explore to what extent microbubbles in the liquid might influence the results and complicate the analysis of the data that are obtained. The existence of microbubbles with diameters ranging from zero to a maximum value of 10^{-5} cm has been shown to be consistent with observed thresholds of sonically induced cavitation in liquids, and we shall assume the existence of such bubbles in this analysis. Theoretical studies dealing with the formation, the stability, and the dynamics of such bubbles have been made by numerous investigators, and will not be considered in the present discussion.

For sound waves in the kilomegacycle region the wavelength is one order of magnitude larger than the largest bubbles in the range mentioned here. The sound pressure then is approximately uniform about a bubble and will drive the bubble in a purely radial pulsating mode of motion. The radiative reaction of the surrounding liquid to this motion provides both damping and a mass load, and the response of the bubble to the sound field is equivalent to that of a resonator. The resonance frequency is determined by the radiative mass load and the effective compressibility; this represents the

*This work was supported by the U.S. Navy (Office of Naval Research) under Contract N00014-67-A-0204-0019.

combined effects of compressibility of the gas in the bubble and surface tension.

If we introduce a (complex) compressibility K in the equations of motion for a viscous fluid carrying a sound wave of the form exp(ikx-iωt), the propagation constant k can be expressed as

$$k^2 = \omega^2 \left(\frac{1}{K\rho} - i\omega\nu\right)^{-1}, \tag{1}$$

where ρ is the density of the fluid, and $(3\nu/4)$ is the kinematic viscosity. The compressibility K includes the effects of heat conduction and various molecular relaxation phenomena, and also the effect of bubbles and other possible impurities. These effects are additive in the compressibility, and we can set

$$K = \frac{1}{\rho c_o^2}\left[1+R(\omega)+B(\omega)\right], \tag{2}$$

where c_o is the low-frequency value of the speed of sound in the pure liquid; the complex quantity $R(\omega)$ accounts for relaxation effects and heat conduction; and B for the effect of the bubbles. In general, these effects are not additive in the expression for the propagation constant:

$$(k/k_o)^2 = \left\{\left[1+R(\omega)+B(\omega)\right]^{-1} - ik_o\ell\right\}^{-1}, \tag{3}$$

in which $k_o = \omega/c_o$, and the characteristic length $\ell = \nu/c_o$ is the liquid equivalent of the mean-free path in a gas. Thus, as far as acoustic dispersion is concerned, there is always some coupling between viscosity and the various mechanisms affecting compressibility. Separation of these effects is meaningful only when they are sufficiently small that R, B, and $(k_o\ell)$ are all small compared with unity. We consider here only this last case, and the expression for k then reduces to

$$k/k_o \approx 1 + \frac{1}{2}(R+B+ik_o\ell). \tag{4}$$

The processes contributing to R have been studied extensively; we shall deal only with the B-term, which we think is responsible for the observed resonant behavior of the dispersion curve.

The microbubbles are assumed to range in size from zero to a maximum value, that is, $0 < r_o \leq r_m$, where r_o is the bubble radius. Starting from the equilibrium condition for a bubble, $P_i = P_o + (2\sigma/r_o)$ with P_i the bubble gas pressure, P_o the static liquid pressure, and σ the surface tension, and accounting for the effect of the radiative mass load of a pulsating bubble, we find that the bubble resonance frequency is given by

$$\omega_o = \sqrt{\frac{(3\gamma-1)2\sigma}{r_o^3\rho}} = \omega_m \left(\frac{r_m}{r_o}\right)^{3/2}. \tag{5}$$

To obtain this relation, we have made three assumptions: $P_i \gg P_o$, which is valid for the microbubbles considered here; the compression of the gas in the bubble is adiabatic; and the bubble radius is small compared with the acoustic wavelength. For the distribution of bubble sizes assumed, the resonance frequencies of the bubbles range from the value ω_m and up, where ω_m is the resonance frequency of the bubble size with the largest radius r_m. Considering water with a surface tension σ = 73 dyn/cm, we find that if we choose a bubble radius of approximately 5×10^{-6} cm, which is consistent with the bubble size required to explore observed cavitation thresholds in sonically induced cavitations, we obtain a resonance frequency of $\sim 10^9$ Hz, which is in the region occurring in Brillouin scattering studies. Thus, if a resonance type of dispersion were to be found in such studies, we propose that a possible explanation might be the existence of microbubbles.

To calculate the function $B(\omega)$, let $\delta \cdot n(\omega_o)d\omega_o$ be the number of bubbles per unit volume in the frequency range between ω_o and $(\omega_o + d\omega_o)$, where δ is the total volume occupied by all bubbles per unit volume of the fluid. The distribution function $n(\omega_o)$ then satisfies the normalization condition $\int_{\omega_m}^{\infty} n(\omega_o)\, v_o\, d\omega_o = 1$, where v_o is the bubble volume. Making use of $\delta \ll 1$, we find that the bubble contribution B in the dispersion relation (4) can be expressed as

$$B = \frac{3\delta}{(\omega_m \tau)^2}\left[\alpha(\gamma, \omega_m, \tau) + i\beta(\gamma, \omega_m, \tau)\right], \tag{6a}$$

where $\gamma = \omega/\omega_m$, and τ is the "relaxation time" of the bubble, proportional to the damping. If we account only for the radiation damping, neglecting the viscosity of the liquid, we find $\tau = r_m/c_o$. The functions α and β can be expressed as

$$\alpha(\gamma, \omega_m, \tau) = \int_0^1 \frac{(1-\gamma^2x^2)x^{2/3}\, n(\omega x)\, dx}{(1-\gamma^2x^2)^2 + \left(\gamma^3 x^{8/3}\omega_m\tau\right)^2} \tag{6b}$$

$$\beta(\gamma, \omega_m, \tau) = (\gamma^3\omega_m\tau)\int_0^1 \frac{x^{10/3} n(\omega x)\, dx}{(1-\gamma^2x^2)^2 + \left(\gamma^3 x^{8/3}\omega_m\tau\right)^2}. \tag{6c}$$

In terms of these functions α and β we can now express the effect of the bubbles on the attenuation and the speed of sound. The expressions for the attenuation per wavelength and for the fractional change of the speed of sound are

$$(\lambda \cdot \mathrm{Im}\,(k)) = \frac{3\pi\delta}{(\omega_m \tau)^2}\,\beta(\gamma, \omega_m, \tau) \tag{7}$$

$$\left(\frac{\Delta c}{c_o}\right) = -\frac{3}{2}\,\frac{\delta}{(\omega_m \tau)^2}\,\alpha(\gamma, \omega_m, \tau). \tag{8}$$

To illustrate this analysis, we have computed the frequency dependence of the attenuation and the speed of sound for a special case that should be closely related to the conditions in the reported experiments. Thus we have chosen $(\omega_m/2\pi) \approx 10^9$ Hz and $r_m \approx 4 \cdot 10^{-6}$ cm, which gives $\omega_m \tau \approx 0.1$. Furthermore, we have assumed a bubble distribution function, n, which is zero for $\omega_o < \omega_m$ and constant for $\omega_o > \omega_m$. Our results are shown in Fig. XI-1. These curves have two interesting features. First, we note

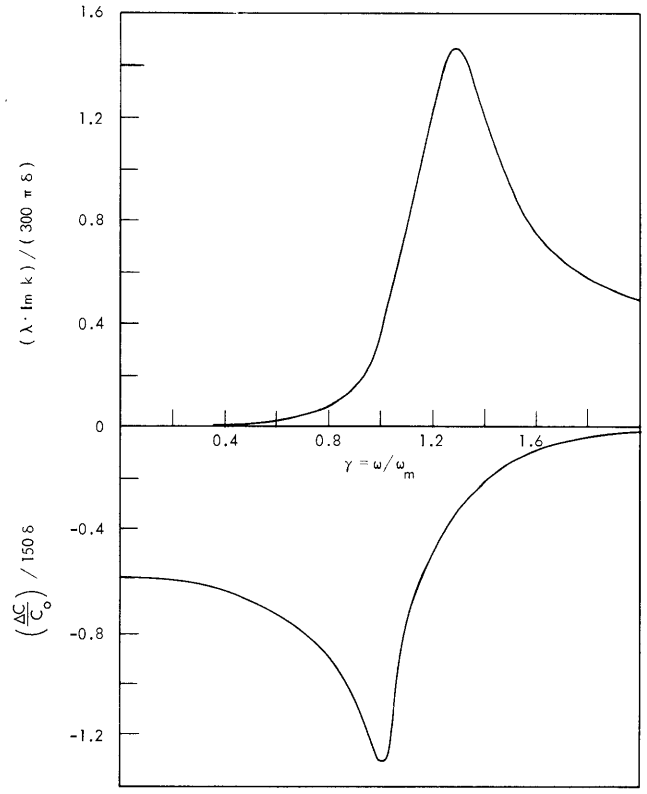

Fig. XI-1. Dispersion relation for high-frequency waves in a liquid with a distribution of microbubbles.

that the peak in the attenuation occurs at a frequency that is markedly greater than ω_m, whereas the peak in the change of the speed of sound occurs at a frequency approximately equal to ω_m. Second, the shape of the curve for $\Delta c/c_o$ is such that after having reached its minimum value it goes back to zero monotonically. For a single resonance, on the

other hand, the curve goes to zero after having passed a maximum value. These two features are in qualitative agreement with experimental results. Note also that the maximum values of the fractional change of the velocity of sound and of the attenuation per wavelength produced by the bubbles are of the same order of magnitude. To obtain a 1% change in $\Delta c/c_o$, the total bubble volume should be approximately five parts in 10^5 for the distribution function and the values of the parameters used in this example.

K. U. Ingard

B. INTERACTION OF ACOUSTIC SURFACE WAVES WITH ELECTRON SURFACE WAVES[†]

We have observed the resonant coupling and amplification of acoustic surface waves on a piezoelectric with electron surface waves on an adjacent semiconductor in a transverse magnetic field.

The sample configuration used in our experiments is shown in Fig. XI-2. The acoustic surface waves, propagating along the Z direction on a Y-cut polished surface

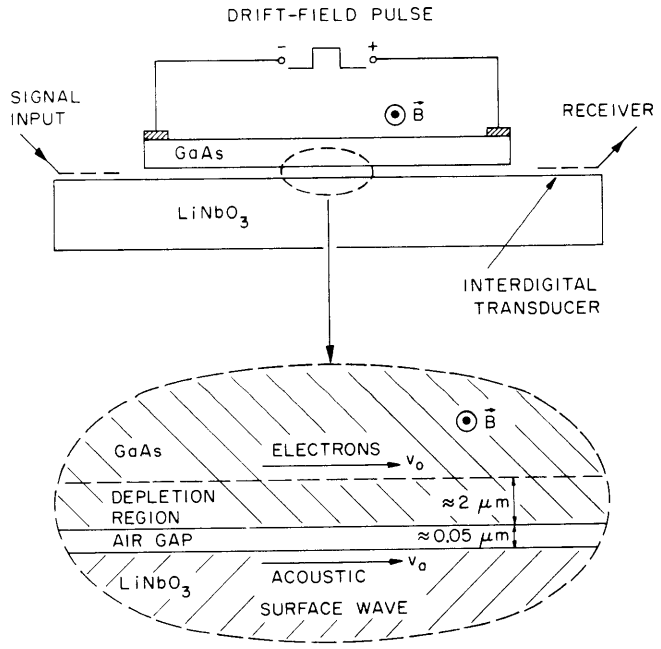

Fig. XI-2. Sample configuration.

[†]This work was supported in part by the National Science Foundation (Grant GK-18185). Part of this work was performed while one of the authors (C. K.) was a Guest Scientist at the Francis Bitter National Magnet Laboratory, M. I. T., which is supported by the Air Force Office of Scientific Research.

of single-crystal $LiNbO_3$, were generated and detected by a pair of interdigital transducers. The interaction length over which the GaAs and $LiNbO_3$ were in close proximity (<1000 Å) was 5 mm. Room-temperature measurements were made at 150 MHz with magnetic fields of up to 144 kG. A low duty-cycle drift-field pulse (10 μs at 25 pps) was used to avoid sample heating problems.

The dispersion relation for the coupled waves, in the case of a semiconductor with a depletion region of depth d that is separated from the piezoelectric by a negligibly small air gap, is given by[1]

$$(k-k_a)(k-k_e) = -\frac{K^2}{2}\frac{\omega}{v_a}\frac{R\omega_\sigma^*}{v_o}(b-j)\frac{(1-Q)}{(1+jbQ)} \tag{1a}$$

$$k_e = \frac{\omega}{v_o} + \frac{R\omega_\sigma^*}{v_o}(b-j)\frac{(1-Q+Q/R)}{(1+jbQ)} \tag{1b}$$

$$\frac{K^2}{2} = \left(\frac{\Delta v}{v}\right)_s \left[\frac{1-\tanh kd}{1+(\epsilon_p/\epsilon_s)\tanh kd}\right] \tag{1c}$$

$$R = \frac{1+(\epsilon_p/\epsilon_s)\tanh kd}{(1+\epsilon_p/\epsilon_s)(1+\tanh kd)} \tag{1d}$$

$$Q = \left[\frac{j\omega/\omega_D^*}{(kv_o/\omega) - 1 + j\left(\omega_\sigma^*/\omega+\omega/\omega_D^*\right)}\right]^{1/2}, \tag{1e}$$

where the coupled-wave fields are assumed to have angular frequency ω and wave number k along the direction of propagation, k_a is the wave number of the acoustic surface wave when the semiconductor conductivity $\sigma_o = 0$, k_e is the wave number of the electron surface wave when $(\Delta v/v)_s$ is zero, K is the effective electromechanical coupling constant, $(\Delta v/v)_s$ is the fraction change in the acoustic phase velocity when σ_o changes from infinity to zero, $\omega_\sigma^* = (\sigma_o/\epsilon_s)(1+b^2)^{-1}$ is the dielectric relaxation frequency, $\omega_D^* = (\omega/k)^2(1+b^2)e/\kappa T\mu$ is the electron diffusion frequency, $b \equiv \mu B$, with μ the electron mobility and B the magnetic field, ϵ_p and ϵ_s are the dielectric constants for the piezoelectric and semiconductor, respectively, v_o is the electron drift velocity, and v_a is the velocity of the acoustic surface wave on the piezoelectric in the absence of the semiconductor.

Figure XI-3 shows the observed acoustic surface-wave attenuation as a function of magnetic field (for both positive and negative polarities), with no applied drift field. The theoretical curves were calculated from Eq. 1 using the following values chosen to fit

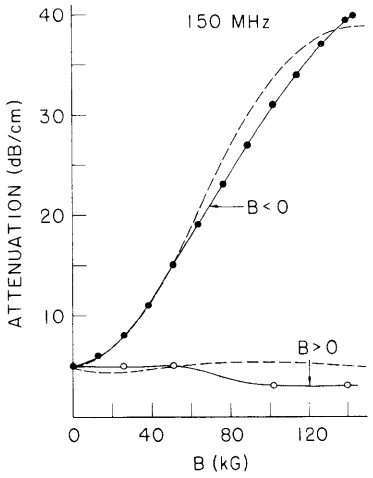

Fig. XI-3.

Attenuation of a 150-MHz acoustic surface wave as a function of magnetic field, with no applied drift field. The theoretical curves are shown as dotted lines.

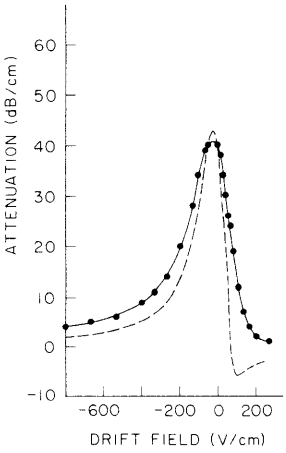

Fig. XI-4.

Attenuation of a 150-MHz acoustic surface wave as a function of applied drift field, with B = -140 kG. The theoretical curve is shown as a dotted line.

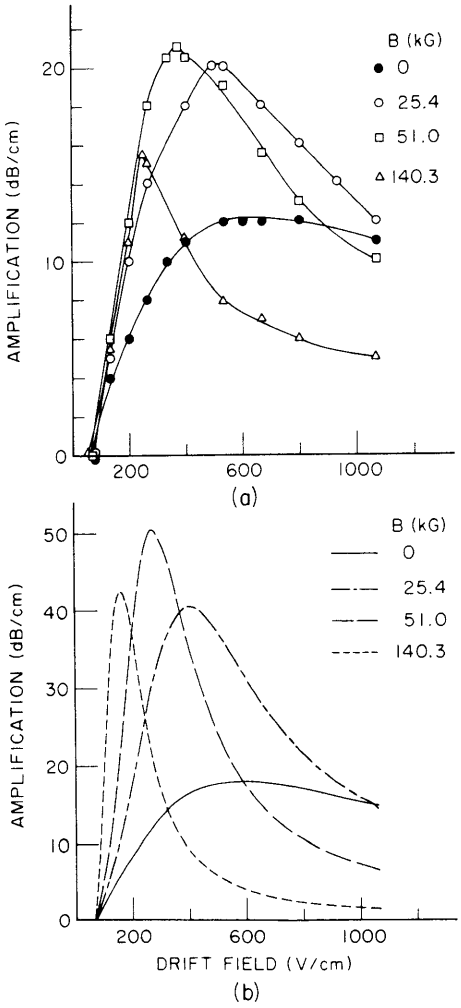

Fig. XI-5.

Amplification of a 150-MHz acoustic surface wave as a function of applied drift field: (a) experimental results, (b) theoretical curves.

the experimental data: an electron mobility $\mu = 5000\ cm^2\ V^{-1}\ s^{-1}$, a free carrier density $n_o = 1.3 \times 10^{13}\ cm^{-3}$, and a depletion-region depth $d = 2.1 \times 10^{-4}$ cm.

For $B < 0$, the acoustic and electric surface waves are coupled positive-energy modes; in our experiments this coupling transfers energy from the generated acoustic wave to the electron wave. Figure XI-4 shows the observed acoustic surface-wave attenuation as a function of drift field, with B = -140 kG.

For $B > 0$, the electron surface wave has a negative small-signal energy and hence can amplify the acoustic wave. Figure XI-5 shows the qualitative agreement between the observed acoustic amplification and the corresponding theoretical curves. The discrepancies may be caused by the resistivity inhomegeneities which were known to exist in the sample, and by electron trapping effects.[2]

C. Krischer, A. Bers

References

1. A. Bers and B. E. Burke, Appl. Phys. Letters 16, 300 (1970); 17, 47 (1970).
2. I. Uchida, T. Ishiguro, Y. Sasaki, and T. Suzuki, J. Phys. Soc. Japan 19, 674 (1964).

C. TECHNIQUES FOR MEASURING DENSITY FLUCTUATIONS IN JETS

Our investigation of various techniques of measuring the density distribution in a supersonic jet has been continued[1] with particular emphasis on the corona probe.

We have used this probe to measure the static density distribution in an Argon jet. The result is qualitatively quite similar to that obtained from the Langmuir-probe measurements of the electron distribution in a weakly ionized jet shown in Fig. XI-6. The variation of the electron density in the jet is large enough to make the jet clearly visible (Fig. XI-6a). The actual measured density variations along and across the jet are shown in Fig. XI-6b and 6c.

During these measurements we found that there was reason to believe that the vertical plane to which our travelling probe is confined may not go through the center of the jet along the entire length of the jet. To make sure that perfect alignment can be obtained, we are now rebuilding the nozzle feed-through into the test chamber so that the jet can be easily aligned. A quantitative analysis of the results will be postponed until they have been repeated with a perfectly aligned jet.

After having obtained the static density distribution in the jet, our objective is to measure also the spectrum of the density fluctuations. To do this, a dynamic calibration of the probe is required. A tentative method of calibration using a sound wave in Argon at a pressure of 10 mm Hg has been tried. Using

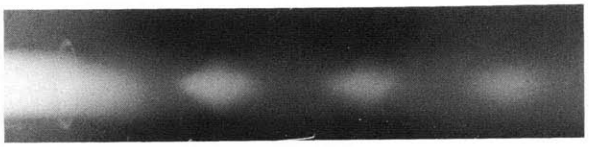

(a)

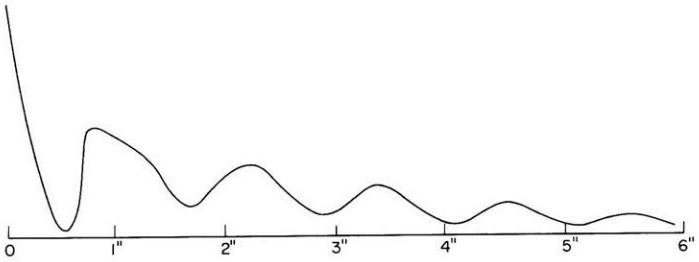

(b)

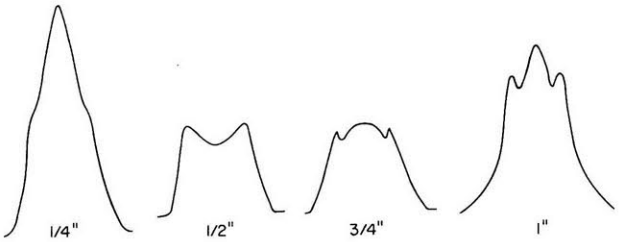

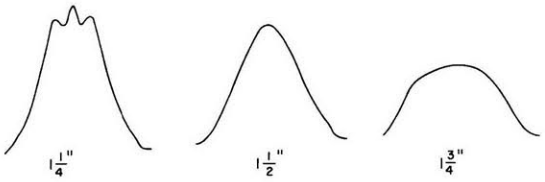

(c)

Fig. XI-6. (a) Supersonic jet from circular nozzle. Argon. Upstream pressure 20 mm. Downstream pressure 0.5 mm.
(b) Electron density along the supersonic jet.
(c) Electron density across the jet at different distances from nozzle.

a small (1-in.) dynamic speaker as a sound source, we were able to detect sound with the corona probe up to frequencies of 500 kHz. An absolute calibration has not yet been obtained.

R. H. Price, U. Ingard

References

1. R. H. Price and U. Ingard, "Techniques for Measuring Density Fluctuations in Jets," Quarterly Progress Report No. 99, Research Laboratory of Electronics, M.I.T., October 15, 1970, pp. 63-64.